# NORTHWESTERN UNIVERSITY

## DEPARTMENT OF MATERIALS SCIENCE

TECHNICAL REPORT # 26

AUGUST 1988

OFFICE OF NAVAL RESEARCH

CONTRACT NO. N00014-80-C-116

SEPARATION OF THE MACRO - and MICRO-STRESSES IN PLASTICALLY DEFORMED 1080 STEEL

BY

R. A. WINHOLTZ and J. B. COHEN





EVANSTON, ILLINOIS

# Separation of the Macro- and Micro-Stresses in Plastically Deformed 1080 Steel



R.A. Winholtz and J.B. Cohen

Department of Materials Science and Engineering
The Technological Institute
Northwestern University
Evanston, IL 60208



## Abstract

The stress tensors were measured with x-ray diffraction in both the ferrite and cementite phases of a 1080 steel specimen deformed in uniaxial tension. The macro- and micro-stresses were separated for all the components of the stress tensors. All the components except the hydrostatic components of the micro-stresses could be determined without an accurate value of the unstressed lattice parameter. Tensile stresses were found in the cementite and compressive stresses in the ferrite along the deformation direction. The tensile stresses in the cementite were quite large. (RW)

## INTRODUCTION

Stresses have long been measured in the matrix phase of steels with diffraction. Steels, however, are generally two-phase materials containing carbides to enhance the properties of the material. Because the diffraction peaks from the carbide phase are so weak, the stresses in this phase and the stress system set up by its presence have not often been examined[1,2]. Recently, theories have been developed and used to investigate the stress system set up in a two-phase material[3,4]. The sensitivity of triaxial stress

measurements to errors in $d_o$, the unstressed lattice parameter, has been a drawback to their use[5]. In this work diffraction measurements of the stresses in both the cementite and ferrite phases of a 1080 steel will be described, as well as an analysis method that eliminates the sensitivity to $d_o$.

## THEORY

### Macro- and Micro-stresses in a Two-Phase Material

In an inhomogeneous material, the stresses from point to point will be different from those predicted by assuming the material to be homogeneous. Almost all engineering materials are inhomogeneous on a small scale and hence will have stresses different than those calculated from a simple theory. In a two-phase material the stresses will not distribute themselves uniformly between the two phases. This gives rise to macro- and micro-stresses within the material.

Macro-stresses vary slowly compared to a part's dimensions in at least one direction, and are by definition the same in both phases of a two-phase material. These stresses may originate, for instance, due to surface layers of a piece elongating more than the interior, for example during peening. Micro-stresses are the difference between the total stress at a point and the macro-stress value. Micro-stresses arise from microstructural properties that cause the stresses to deviate from the macro-stress value from point to point such as the yielding of one phase preferrentially to the other, or differences in the elastic response of two phases mutually constraining each other. The total stress at any point is the sum of these components[6]. For example:

$$ {}^{t}\sigma^{\alpha}_{ij} = {}^{M}\sigma_{ij} + {}^{\mu}\sigma^{\alpha}_{ij} \quad . \tag{1} $$

The superscripts t, M, and $\mu$ refer to the total, macro-, and micro-stresses respectively. The total stress in a phase is the quantity determined from a diffraction measurement on a crystalline material, but on occasion it may be important to separate this into its macro- and micro-stress components. This separation is now discussed.

## Equilibrium Conditions

Stresses in a material must obey several equations of equilibrium. Both the macro-stress and micro-stress at any point must obey the differential equation of equilibrium[3]

$$\frac{\partial {}^{M}\sigma_{11}}{\partial x_1} + \frac{\partial {}^{M}\sigma_{12}}{\partial x_2} + \frac{\partial {}^{M}\sigma_{13}}{\partial x_2} = 0 \quad . \tag{2}$$

The macro- and micro-stresses ${}^{M}\sigma_{13}$, ${}^{M}\sigma_{23}$, and ${}^{M}\sigma_{33}$ must be zero at a free surface to satisfy the boundary conditions. If we can assume that the macro-stresses ${}^{M}\sigma_{11}$ and ${}^{M}\sigma_{12}$ do not vary in the surface Equation 2 requires that the macro-stress ${}^{M}\sigma_{13}$ cannot vary with depth. Since it must be zero at the surface ${}^{M}\sigma_{13}$ is everywhere zero. The same hold true for ${}^{M}\sigma_{23}$ and ${}^{M}\sigma_{33}$. The micro-stresses ${}^{\mu}\sigma^{\alpha}_{13}$, ${}^{\mu}\sigma^{\alpha}_{23}$, and ${}^{\mu}\sigma^{\alpha}_{33}$ are not required to follow this condition for equilibrium because the gradients in the surface are not required to be zero. From the requirement that the average stress over the whole body must be zero,

$$\int_D {}^{t}\sigma_{ij}\, dD = 0 \quad , \tag{3}$$

it can be shown that the average micro-stresses in a two-phase material must obey the relation[3]

$$(1-f)\langle {}^{\mu}\sigma^{\alpha}_{ij} \rangle + f\langle {}^{\mu}\sigma^{\beta}_{ij} \rangle = 0 \quad , \tag{4}$$

where f is the volume fraction of the $\beta$ phase. Since a diffraction measurement samples a volume of material the stresses measured will be an average over that volume. Using Equation 1 for the stresses in each phase. and Equation 4, we have three equations in three unknowns, and hence we may separate the macro- and average micro-stresses.

## Determination of Stresses with Diffraction

To measure stresses with diffraction we establish two coordinate systems as shown in Figure 1. The d-spacing is measured with diffraction in the L-coordinate system along the $L_3$ direction . The stresses in the S-coordinate system are then to be determined with these measurements. The strain along the $L_3$ axis in terms of the sample stresses is[7]

$$\langle \epsilon^{\alpha}_{\phi\psi} \rangle = \frac{d^{\alpha}_{\phi\psi} - d^{\alpha}_{o}}{d^{\alpha}_{o}} = \langle {}^{t}\sigma^{\alpha}_{11} \rangle S^{\alpha}_{2}/2 \cos^2\phi \sin^2\psi + \langle {}^{t}\sigma^{\alpha}_{22} \rangle S^{\alpha}_{2}/2 \sin^2\phi \sin^2\psi$$

$$+ \langle {}^{t}\sigma^{\alpha}_{33} \rangle S^{\alpha}_{2}/2 \cos^2\psi \; ( \langle {}^{t}\sigma^{\alpha}_{11} \rangle + \langle {}^{t}\sigma^{\alpha}_{22} \rangle + \langle {}^{t}\sigma^{\alpha}_{33} \rangle ) S^{\alpha}_{1}$$

$$+ \langle {}^{t}\sigma^{\alpha}_{12} \rangle S^{\alpha}_{2}/2 \sin 2\phi \sin^2\psi + \langle {}^{t}\sigma^{\alpha}_{13} \rangle S^{\alpha}_{2}/2 \cos\phi \sin 2\psi$$

$$+ \langle {}^{t}\sigma^{\alpha}_{23} \rangle S^{\alpha}_{2}/2 \sin\phi \sin 2\psi \quad . \tag{5}$$

By measuring $d_{\phi\psi}$ at a sufficient number of $\phi$, and $\psi$ values and knowing $d_o$. the stresses in the sample coordinate system may be obtained by a least squares solution of this equation[8]. However, an accurate value of $d_o$ must be available to determine the stresses accurately. This problem can be ameliorated by substituting

$$\langle {}^{t}\sigma^{\alpha}_{ij} \rangle = \begin{bmatrix} \langle {}^{t}\tau^{\alpha}_{H} \rangle & 0 & 0 \\ 0 & \langle {}^{t}\tau^{\alpha}_{H} \rangle & 0 \\ 0 & 0 & \langle {}^{t}\tau^{\alpha}_{H} \rangle \end{bmatrix} + \begin{bmatrix} \langle {}^{t}\tau^{\alpha}_{11} \rangle & \langle {}^{t}\tau^{\alpha}_{12} \rangle & \langle {}^{t}\tau^{\alpha}_{13} \rangle \\ \langle {}^{t}\tau^{\alpha}_{12} \rangle & \langle {}^{t}\tau^{\alpha}_{22} \rangle & \langle {}^{t}\tau^{\alpha}_{23} \rangle \\ \langle {}^{t}\tau^{\alpha}_{11} \rangle & \langle {}^{t}\tau^{\alpha}_{12} \rangle & \langle {}^{t}\tau^{\alpha}_{13} \rangle \end{bmatrix} , \tag{6}$$

where $\tau_H$ is the hydrostatic stress and $\tau_{ij}$ is the deviatoric stress tensor.

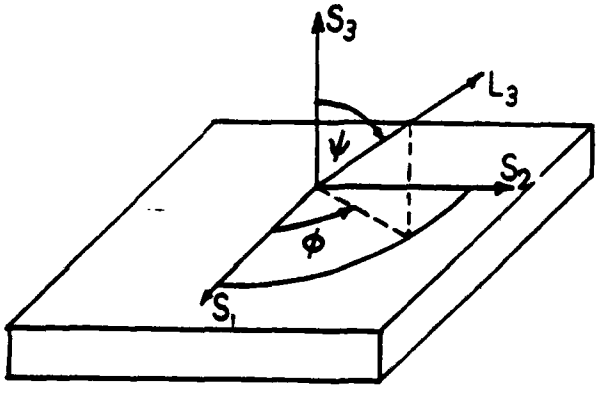


Fig. 1. Definitions of the coordinate systems used to determine stresses with diffraction.

Making use of the relation

$$( {}^{t}\tau^{\alpha}_{11} + {}^{t}\tau^{\alpha}_{22} + {}^{t}\tau^{\alpha}_{33} ) = 0 \quad , \tag{7}$$

which applies to both the stress at a point and averaged stresses, and solving for $\langle d_{\phi\psi} \rangle$ gives the equation

$$\begin{aligned} \langle d^{\alpha}_{\phi\psi} \rangle = {} & \langle {}^{t}\tau^{\alpha}_{H} \rangle d^{\alpha}_{o} [S^{\alpha}_{2}/2 + 3S^{\alpha}_{1}] - ( \langle {}^{t}\tau^{\alpha}_{11} \rangle + \langle {}^{t}\tau^{\alpha}_{22} \rangle ) d_{o} S^{\alpha}_{2}/2 + d_{o} \\ & + \langle {}^{t}\tau^{\alpha}_{11} \rangle d_{o} S^{\alpha}_{2}/2 \, (1 + \cos^{2}\phi) \sin^{2}\psi \\ & + \langle {}^{t}\tau^{\alpha}_{22} \rangle d_{o} S^{\alpha}_{2}/2 \, (1 + \sin^{2}\phi) \sin^{2}\psi \\ & + \langle {}^{t}\tau^{\alpha}_{12} \rangle d_{o} S^{\alpha}_{2}/2 \, \sin 2\phi \, \sin^{2}\psi \\ & + \langle {}^{t}\tau^{\alpha}_{13} \rangle d_{o} S^{\alpha}_{2}/2 \, \cos\phi \, \sin 2\psi \\ & + \langle {}^{t}\tau^{\alpha}_{23} \rangle d_{o} S^{\alpha}_{2}/2 \, \sin\phi \, \sin 2\psi \quad . \end{aligned} \tag{8}$$

Written in this way we see that the d-spacing has five terms with different angular dependencies and three terms that are angularly independent. From a collection of $\langle d_{\phi\psi} \rangle$ the six deviatoric components of the total stress tensor may be determined by least squares using Equation 8 and then using Equation 7. By using Equations 7 and 8 instead of Equation 5, we eliminate the need for an accurate $d_o$ in the analysis, but still need information about the hydrostatic stresses.

Only the sum of the three constant terms may be determined by least squares, and an accurate value of $d_o$ appears necessary to determine the hydrostatic component of the stress. If we take values that might be typical for the ferrite phase in a steel:

$$S_2/2 = 5.77 \times 10^{-6} \text{ MPa}^{-1}$$

$$S_1 = -1.25 \times 10^{-6} \text{ MPa}^{-1}$$

$$d_o = 1.1703 \text{ Å}$$

and an error in $d_o$ of 0.0001 Å, we see that an error in the hydrostatic stress of 42 MPa is needed to keep the sum of the three terms on the left hand side of Equation 8 a constant. (This corresponds to an error in of 0.03° $2\theta$ at 156° $2\theta$ in determining $d_o$.)

By using least-squares fitting and Equations 7 and 8 we may determine the total deviatoric stress tensor ${}^{t}\tau^{a}_{ij}$ in a phase from a collection of d vs. $\phi$ and $\psi$ for that phase. Using Equations 1 and 4 we may separate the total stress tensors into the macro- and average micro-stress tensors for each component of the stress tensors. Then, if an accurate value of $d_o$ is not available for each phase, the hydrostatic component of the macro-stress tensor may still be determined. We know from the equilibrium relations that ${}^{M}\sigma_{33}$ must be zero. We may thus write

$$ {}^{M}\sigma_{33} = {}^{M}\tau_{H} + {}^{M}\tau_{33} = 0 \quad . \tag{9} $$

The hydrostatic macro-stress is then

$$ {}^{M}\tau_{H} = -{}^{M}\tau_{33} \quad . \tag{10} $$

Thus, without accurate values of $d_o$, we may determine all the components of the macro-stress tensor and all the components of the micro-stress tensors in both phases except for the average hydrostatic micro-stress in each phase.

## Experimental

Samples were cut from a plate of hot rolled 1080 steel. Heat treatment consisted of austenitizing in Argon at 1073 K for 15 minutes followed by a slow cool (in Argon) outside of the hot zone of the furnace. This heat treatment produced a pearlitic microstructure in the sample. The sample was then pulled in tension to a true plastic strain of 0.118. The final stress on the sample when it was released was 818 MPa.

Cementite has an orthorhombic crystal structure[9], which gives rise to many diffraction peaks, none of which are terribly strong. Not coincidently, the strongest diffraction peaks are often near to the ferrite peaks and overlap a considerably.

In order to obtain sufficient diffracted intensity from the carbide phase, a chromium rotating anode x-ray target was constructed. A copper target was chrome plated to a thickness of 0.001 inches in the area that the electrons strike it, so that chromium characteristic radiation would be

produced. Chromium is widely used for stress analysis on steel because it gives a ferrite peak at a high angle. For the cementite, the long wavelength chromium radiation has the benefit of keeping the many peaks from bunching up and overlapping each other and keeps the distance in reciprocal space low so that the peak broadening is minimized. The x-ray generator was run at 47.5 kV and 200 mA for the measurements. Diffraction measurements were carried out on a Picker diffractometer with a quarter-circle goniometer and a graphite diffracted beam monochromator. The monochromator was needed to reduce the background counts so that a good peak to background ratio was obtained for the carbide peak. Psi goniometry was used to obtain the necessary $\psi$-tilts[10].

The 211 ferrite peak at about 156° $2\theta$ was used for the stress measurements in the ferrite phase, while the 250 cementite peak at about 148° $2\theta$ was used for the stress measurements in the carbide phase. Figure 2 shows the relative intensities of the ferrite and carbide peaks at $\phi$ and $\psi$ equal to zero. The ferrite peaks were measured by counting 20 seconds at each point while the cementite peaks were counted for 300 seconds a point. The total measurement time for all the peaks measured was about 120 hours.

The sample was mounted on the diffractometer such that the tensile deformation axis corresponded to the direction $\phi = 0$. The peaks were point counted and fitted with pseudo-Voigt functions[11] including both the $K_{\alpha_1}$ and $K_{\alpha_2}$ components. The peak positions were then obtained from the functional parameters. For the ferrite peaks, a linear background was assumed, while for the cementite peaks the background was assumed to be an exponential function plus a constant, because the 250 carbide peak sits on the tail of the 211 ferrite peak. Figure 3 shows the functional fit to the cementite diffraction peak at $\psi$=0. Peak positions were determined in both phases over a $\psi$ range of -45 to +45 degrees for $\phi$ equal to 0, 60, and 120 degrees.

The volume fraction of the carbide phase was determined from the ratio of the integrated intensity of the 121, 210, 112, 211, and the 250 carbide peaks to the intensity of the 100, 110, and the 211 ferrite peaks[12]. It was found to be 11 $\pm$ 2 percent. Averaging over a number of peaks helps to eliminate any errors due to preferred orientation. This measurement is consistent with the volume percent expected for a 1080 steel.

(a)

(b)

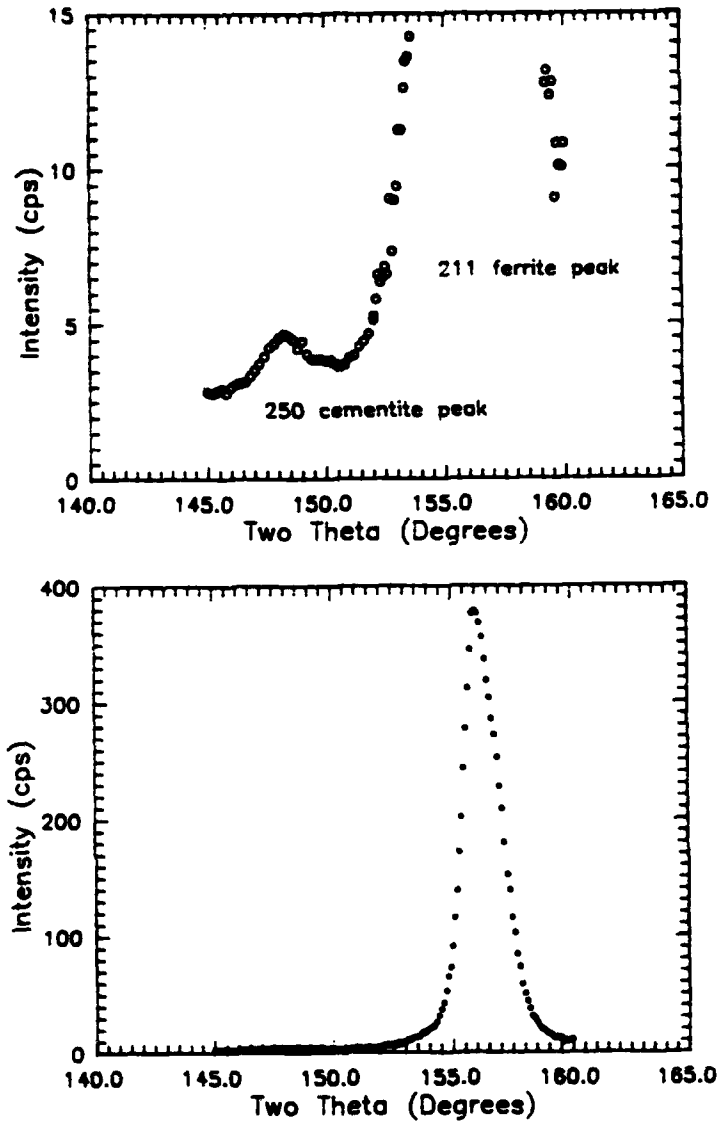


Fig. 2. Diffraction peaks used for the stress analysis at $\psi = 0$, empasizing the ferrite peak (a) and the cementite peak (b).

## RESULTS AND DISCUSSION

Figure 4 shows a plot of d vs. $\sin^2\psi$ for both phases at $\phi = 0$. The stress tensors were determined from the above analysis to be

$$\mu_T{}^C = \begin{bmatrix} 445 & 59 & 7 \\ 59 & -304 & 20 \\ 7 & 20 & -142 \end{bmatrix}$$

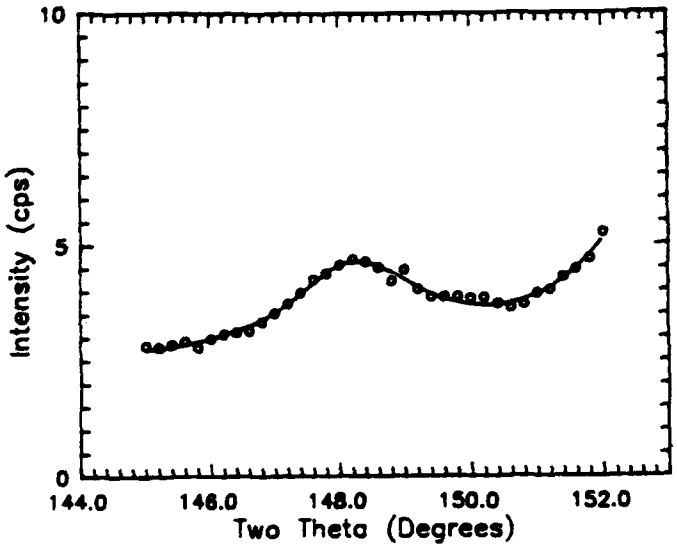


Fig. 3. Psuedo-Voigt functional fit to cementite peak for $\psi = 0$.

$$\mu_T{}^{\alpha} = \begin{bmatrix} -55 & -7 & -1 \\ -7 & 38 & -2 \\ -1 & -2 & 17 \end{bmatrix}$$

$$M_{\sigma} = \begin{bmatrix} -39 & 5 & 2 \\ 5 & -28 & 0 \\ 2 & 0 & 0 \end{bmatrix}$$

A value of $5.77 \times 10^{-6}$ MPa$^{-1}$ was used for $S_2/2$ for the ferrite phase[13]. This same value was used for the cementite phase as no better value is as yet available.

The deviatoric micro-stress ${}^{\mu}\tau_{11}^{c}$ along the deformation axis are tensile and very big in the carbide phase and the corresponding stress is compressive in the ferrite phase. The large tensile stress in the cementite is important to note as it could lead to crack initiation. The deviatoric micro-stresses perpendicular to the deformation direction ${}^{\mu}\tau_{22}^{c}$ and ${}^{\mu}\tau_{33}^{c}$ are smaller

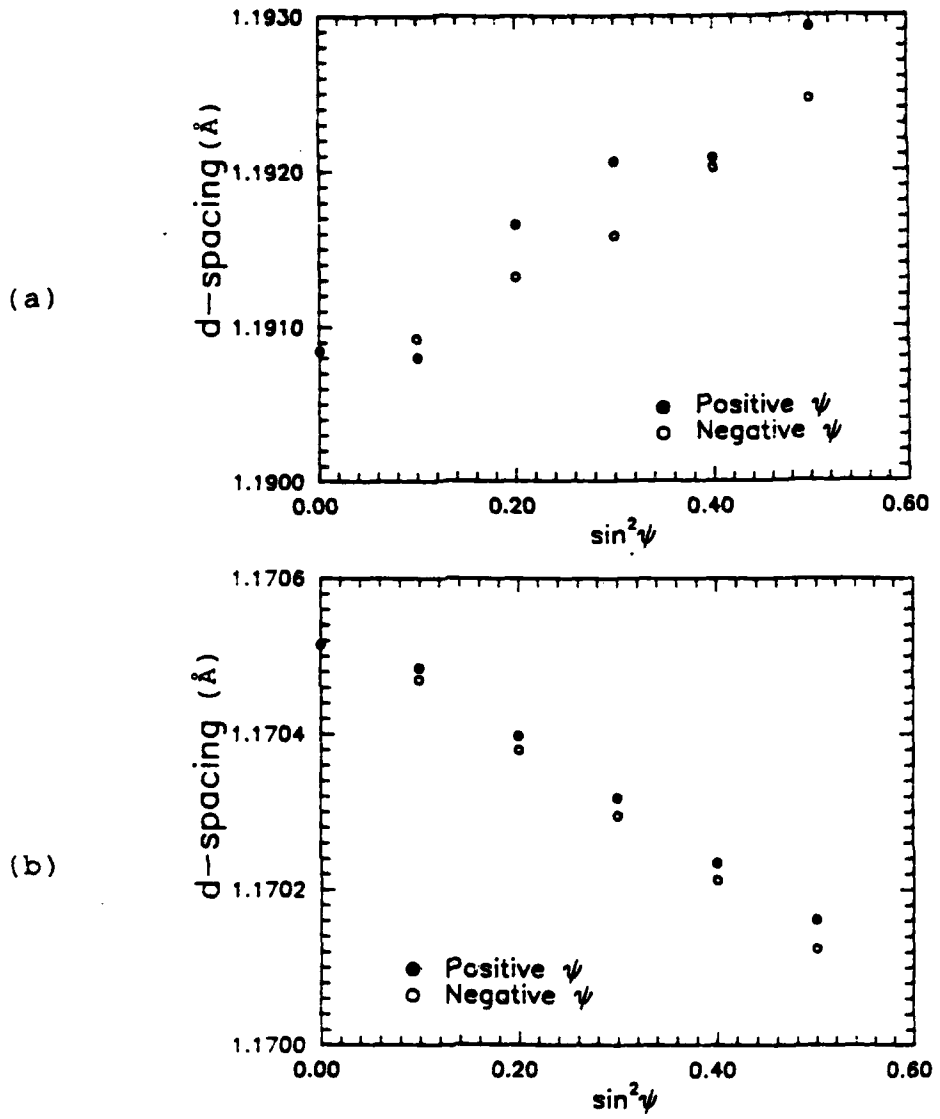


Fig. 4. d vs. $\sin^2\psi$ plots for the cementite (a) and ferrite (b) phases.

and opposite to ${}^{\mu}\tau^{c}_{11}$. This is consistent with the deformation of a harder carbide phase in a softer ferrite matrix. The value of ${}^{\mu}\tau^{c}_{33}$ is smaller and consistent with the fact that this stress must be zero at the surface and the measured value is an average over the penetration depth of the x-rays. The macro-stress ${}^{M}\sigma_{33}$ is zero because it was set to that value to do the analysis. The non-zero value of ${}^{M}\sigma_{13}$ is probably indicative of the errors in the measurements.

The hydrostatic stress ${}^{M}\tau_{H}$ is shown as a function of the value of $d^{c}_{o}$ used in Figure 5. For comparison the hydrostatic micro-stress, ${}^{\mu}\tau^{c}_{H}$, is also

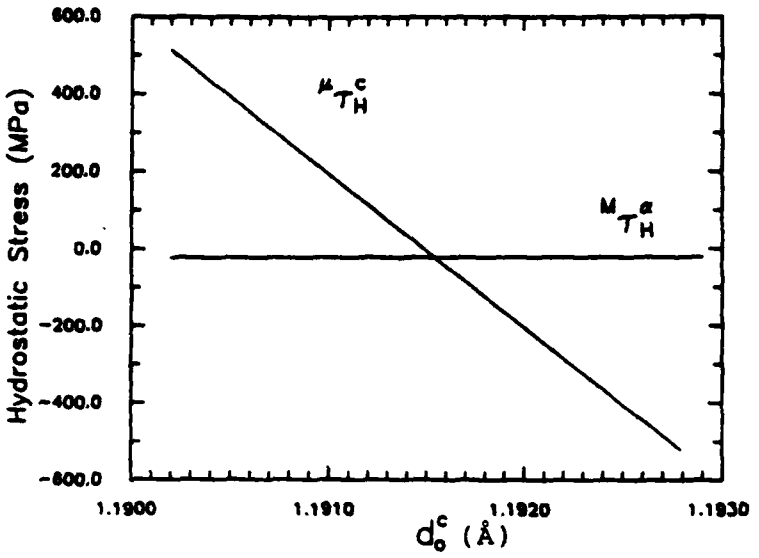


Fig. 5. The hydrostatic stresses $^{\mu}T_H^c$ and $^{M}T_H^{\alpha}$ as a function of the unstressed d-spacing $d_o^c$ used.

shown. The range of $d_o^c$ used was the range of d-spacings found in the data. We see that the hydrostatic macro-stress is indeed insensitive to the value of $d_o^c$, while the hydrostatic micro-stress in the cementite phase varies considerably. Using the lattice parameters in Reference 9 to determine $d_o^c$ gives a hydrostatic macro-stress of -22 MPa and a hydrostatic microstress of -44 MPa in the cementite phase. This would require the hydrostatic micro-stress in the ferrite phase to be 5 MPa to satisfy Equation 4.

## SUMMARY

1) A chromium rotating anode target was constructed, which was used to generate sufficient incident intensity to allow the measurement of stresses in the cementite phase of a steel using the 250 reflection.

2) The sensitivity of a measured triaxial stress tensor to the value of the unstressed lattice parameter was revealed to be an inability to determine the hydrostatic component of the stress tensor.

3) By making diffraction measurements in both phases of a two phase material the deviatoric components of the macro- and micro-stresses can be determined, as well as the hydrostatic component of the macro-stress

without accurate values of the unstressed lattice parameters. This leaves only the hydrostatic component of the micro-stresses undeterminable without the unstressed lattice parameters.

4) The macro- and average micro-stresses in a pearlitic 1080 steel sample plastically deformed in tension were determined using the above procedures. The results are consistent with a the stresses expected when a soft matrix with a hard second phase is deformed. The ferrite is in compression along the deformation axis and the cementite in tension. The large value of the latter stress could lead to crack initiation.

## ACKNOWLEDGEMENTS

This research was supported by the Office of Naval Research under contract No. N00014-80-C-116.

## REFERENCES

1. D.V. Wilson and Y.A. Konnan, Work hardening in a steel containing a coarse dispersion of cementite particles, Acta Met. 12:617 (1964).

2. T. Hanabusa, J. Fukura, and H. Fujiwara, X-ray stress measurement on the cementite phase in steels, Bull. JSME 12:931 (1969).

3. I.C. Noyan, Equilibrium conditions for the average stresses measured by x-rays, Met. Trans. A 14A:1907 (1983).

4. I.C. Noyan and J.B. Cohen, An x-ray diffraction study of the residual stress-strain distributions in shot-peened two-phase brass, Mat. Sci. Engr. 75:179 (1985).

5. I.C. Noyan, Determination of the usnstressed lattice parameter "$a_o$" for (triaxial) residual stress determination by x-rays, Adv. X-Ray Anal. 28:281 (1985).

6. J.B. Cohen, The measurement of stresses in composites, Powder Diffraction 1:15 (1986).

7. H. Dölle, The influence of multiaxial stress states, stress gradients and elastic anisotropy of the evaluation of (residual) stresses by x-rays, J. Appl. Cryst. 12:489 (1979).

8. R.A. Winholtz and J.B. Cohen, A generalised least-squares determination of triaxial stress states by x-ray diffraction and the associated errors, Aust. J. Physics, in press.

9. H. Lipson and N.J. Petch, The crystal structure of cementite, $Fe_3C$, J. Iron Steel Inst., 142:95 (1940).

10. I.C. Noyan and J.B. Cohen, "Residual Stress: Measurement by Diffraction and Interpretation," Springer-Verlag, New York (1987).

11. G.K. Wertheim, M.A. Butler, K.W. West, and D.N.E. Buchanan, Determination of the Gaussian and Lorentzian content of experimental line shapes, Rev. Sci. Instrum., 45:1369 (1974).

12. L.H. Schwartz and J.B. Cohen, "Diffraction from Materials," Springer-Verlag, New York (1987).

13. H. Dolle and J.B. Cohen, Residual stresses in ground steels, Met. Trans. A, 11A:159 (1979).

Security Classification

## DOCUMENT CONTROL DATA - R & D

*(Security classification of title, body of abstract and indexing annotation must be entered when the overall report is classified)*

| | |
|---|---|
| 1. ORIGINATING ACTIVITY *(Corporate author)*<br>J. B. Cohen<br>Northwestern University<br>The Technologial Institute, Evanston, IL 60208 | 2a. REPORT SECURITY CLASSIFICATION<br><br>2b. GROUP |

3. REPORT TITLE

Separation of the Macro and Micro-Stresses in Plastically Deformed 1080 Steel

4. DESCRIPTIVE NOTES *(Type of report and inclusive dates)*

Technical Report #25

5. AUTHOR(S) *(First name, middle initial, last name)*

R. A. Winholtz and J. B. Cohen

| 6. REPORT DATE | 7a. TOTAL NO. OF PAGES | 7b. NO. OF REFS |
|---|---|---|
| August 1988 | 13 | |

| 8a. CONTRACT OR GRANT NO. | 9a. ORIGINATOR'S REPORT NUMBER(S) |
|---|---|
| N00014-80-C-116 | |
| b. PROJECT NO. | 25 |
| c. | 9b. OTHER REPORT NO(S) *(Any other numbers that may be assigned this report)* |
| d. | |

10. DISTRIBUTION STATEMENT

Distribution of document is unlimited

| 11. SUPPLEMENTARY NOTES | 12. SPONSORING MILITARY ACTIVITY |
|---|---|
| | Metallurgy Branch<br>Office of Naval Research |

13. ABSTRACT

The stress tensors were measured with x-ray diffraction in both the ferrite and cementite phases of a 1080 steel specimen deformed in uniaxial tension. The macro and micro-stresses were separated for all the components of the stress tensors. All the components except the hydrostatic components of the micro-stresses could be determined without an accurate value of the unstressed lattice parameter. Tensile stresses were found in the cementite and compressive stresses in the ferrite along the deformation direction. The tensile stresses in the cementite were quite large.

DD FORM 1 NOV 68 1473 (PAGE 1)

S/N 0101-807-6801

Security Classification

| 14. KEY WORDS | LINK A | | LINK B | | LINK C | |
|---|---|---|---|---|---|---|
| | ROLE | WT | ROLE | WT | ROLE | WT |
| Residual stresses in composites<br>Residual stresses in steel<br>Residual stresses in cementite<br>Micro and Macrostresses | | | | | | |